ACSNANO

www.acsnano.org

ARTICLE

Rotating-Disk-Based Hybridized Electromagnetic–Triboelectric Nanogenerator for Sustainably Powering Wireless Traffic Volume Sensors

Binbin Zhang,[†,#] Jun Chen,[‡,#] Long Jin,[†] Weili Deng,[†] Lei Zhang,[†] Haitao Zhang,[†] Minhao Zhu,[†,§] Weiqing Yang,[*,†] and Zhong Lin Wang[*,‡,∥]

[†]Key Laboratory of Advanced Technologies of Materials (Ministry of Education), School of Materials Science and Engineering, and [§]State Key Laboratory of Traction Power, Southwest Jiaotong University, Chengdu 610031, China

[‡]School of Materials Science and Engineering, Georgia Institute of Technology, Atlanta, Georgia 30332, United States

[∥]Beijing Institute of Nanoenergy and Nanosystems, Chinese Academy of Sciences, Beijing, China

Supporting Information

ABSTRACT: **Wireless traffic volume detectors play a critical role for measuring the traffic-flow in a real-time for current Intelligent Traffic System. However, as a battery-operated electronic device, regularly replacing battery remains a great challenge, especially in the remote area and wide distribution. Here, we report a self-powered active wireless traffic volume sensor by using a rotating-disk-based hybridized nanogenerator of triboelectric nanogenerator and electromagnetic generator as the sustainable power source. Operated at a rotating rate of 1000 rpm, the device delivered an output power of 17.5 mW, corresponding to a volume power density of 55.7 W/m^3 ($P_d = P/V$, see Supporting Information for detailed calculation) at a loading resistance of 700 Ω. The hybridized nanogenerator was demonstrated to effectively harvest energy from wind generated by a moving vehicle through the tunnel. And the delivered power is capable of triggering a counter *via* a wireless transmitter for real-time monitoring the traffic volume in the tunnel. This study further expands the applications of triboelectric nanogenerators for high-performance ambient mechanical energy harvesting and as sustainable power sources for driving wireless traffic volume sensors.**

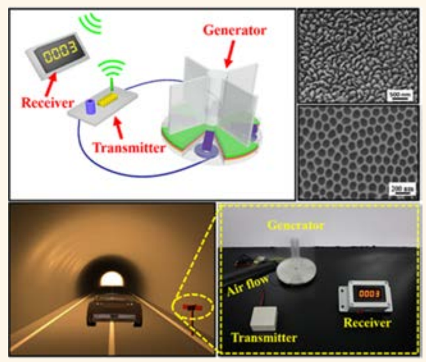

KEYWORDS: *hybridized electromagnetic–triboelectric nanogenerator, self-powered wireless sensor*

Aimed at providing innovative services relating to different modes of transportation and traffic management, the operation of Intelligent Traffic System (ITS) intensely relies on accurate measurement of traffic-flow characteristics. A wireless traffic volume detector plays a critical role of obtaining the timely information on traffic-flow.[1,2] However, the current wireless traffic volume detectors are mainly powered by a traditional power supply unit, such as batteries. Nevertheless, because of the limited lifetime and the potential environmental pollution issue of the batteries, a sustainable and portable power source is highly desired for the traffic volume sensors, especially in remote areas, for real-time traffic volume monitoring.[3−5] Recently, ascribing to a coupling effect of contact electrification and electrostatic induction, the triboelectric nanogenerator (TENG) has been proven to be an effective and robust approach for ambient mechanical energy harvesting.[6−14] Mainly utilizing conventional polymer thin film materials, the TENG has been proven as a fundamentally green energy technology, featured as being simple, reliable, and cost-effective as well as highly efficient, and its performance is superior to other approaches of its kind.[15−24] However, as a complementary energy technology to the traditional electromagnetic generator (EMG), the TENG suffers from a relatively low current output compared to its voltage output, and a hybridization of the two could be a superior solution to this problem. In this regard, here, we designed a rotating-disk-based hybridized nanogenerator of EMG and TENG for high-performance mechanical energy harvesting. With a device diameter of 10 cm and a height of 1 cm at an operational rotation rate of 1000 rpm, the hybridized nanogenerator can produce output powers of 17.5 mW, corresponding to a volume power density of 55.7 W/m^3, and the hybridized nanogenerator was demonstrated to continuously power a wireless traffic volume sensor by harvesting air flow energy aroused by a moving car in the

Received: April 8, 2016
Accepted: May 27, 2016

DOI: 10.1021/acsnano.6b02384
ACS Nano XXXX, XXX, XXX−XXX

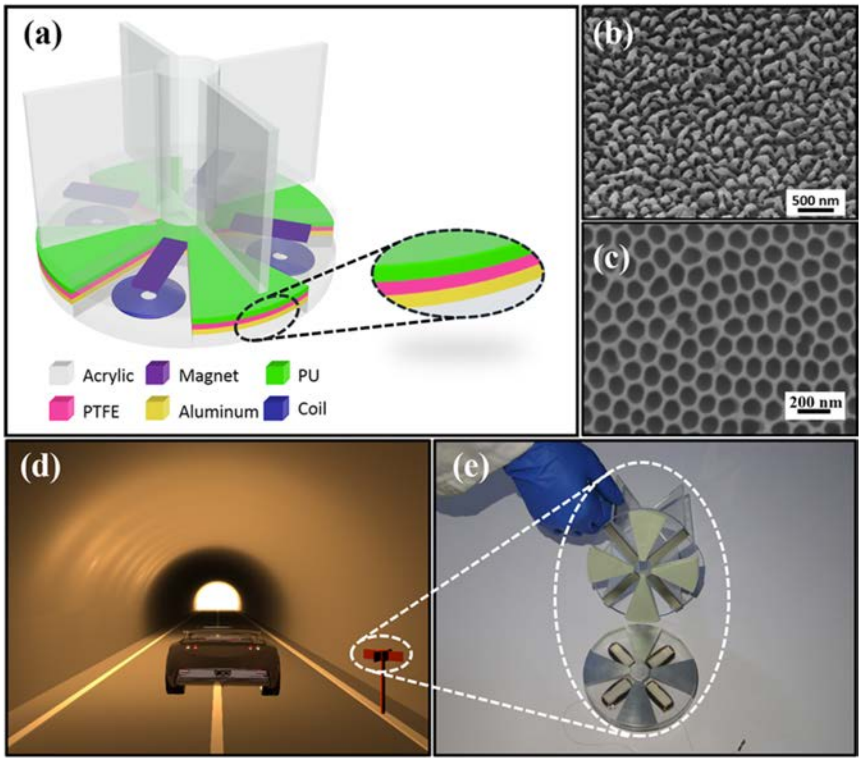

Figure 1. Structural design of self-powered wireless traffic volume system: (a) sketch of the sensor; (b) SEM image of PTFE surface with nanostructure modification; (c) SEM image of aluminum nanopores; (d) schematic diagram of the sensor which is working in the tunnel; (e) enlarged view of the self-power sensing system.

tunnel. This work presents solid progress toward the practical applications of nanogenerators in harvesting ambient mechanical energy for self-powered wireless sensor networks.

RESULTS AND DISCUSSION

The hybridized nanogenerator holds a disk structure with a blade on the top to convert the ambient water/wind flow into mechanical rotational motion, as schematically illustrated in Figure 1a. The hybridized nanogenerator mainly consists of two parts, a rotator and a stator. The rotator is composed of four acrylic intercrossing blades, anchored on a disk acrylic substrate. On the other side of the acrylic substrate, a layer of soft polyurethane (PU) acted as the buffering layer. On top of it, a layer of polytetrafluoroethylene (PTFE) was laminated as one of the triboelectric layers which can easily gain electrons from the Al foil, as shown in Supporting Information, Table S1. And also four bar magnets are uniformly anchored on the rotator plane. When it comes to the stator, four groups of coils, as another part of the EMG, are uniformly distributed on an acrylic substrate. Another layer of aluminum was laminated onto the stator as another triboelectric layer. In addition, to increase the triboelectrification, a surface nanostructure modification was employed to both PTFE and the aluminum surface. As shown in Figure 1b, the inductively coupled plasma (ICP) progress was employed to make nanowires on the surface of the PTFE film by reactive ion etching.[25] And on the surface of aluminum triboelectric layer, nanopores are created with uniform size and distribution, as shown in Figure 1c. For practical application, an integration of the commercial traffic volume sensor with the hybridized nanogenerator will form a self-powered sensing system, which could be installed inside the tunnel, as illustrated in Figure 1d. Figure 1e is an enlarged view of the fabricated device.

The working principle of the hybridized nanogenerator for mechanical energy harvesting is demonstrated in Figure 2. Here, the working principle can be elucidated from two aspects, namely, triboelectric effect based and electromagnetic-effect based electricity generation. Regarding the triboelectrification enabled mechanical energy harvesting, the electricity-generating process is elaborated through a basic unit, as shown in Figure 2a. At the original state (stage I), when the PTFE film was brought to contact with the Al foil, due to the difference of the electron affinity between the two, charge transfer at the interface will make the PTFE negatively charged and aluminum positively charged.[26−33] These tribo-charges will sustain on the materials surface for an extended period of time. In the aligned position, the positive triboelectric charges are fully compensated with the negative ones. Once the rotator starts to spin, a displacement occurs, and the triboelectric charges are not compensated at the displaced areas. The sliding apart of the negatively charged PTFE, will result in a decrease of the induced positive charges on the aluminum, which will create a flow of electrons from the ground to the aluminum (stage II). The flow of induced electrons can last until a new electrical equilibrium is established (stage III). Because of the periodic structure, a further rotation will result in a current in the opposite direction (stage IV). When it comes to the electromagnetic-effect-based mechanical energy harvesting, its working mechanism is clearly displayed in Figure 2b. The distribution of magnetic field was calculated *via* COMSOL. At stage I, the magnets are in alignment with coils and the magnetic flux through the coils is maximized with no current in the coils, and the flux will keep decreasing when the rotator spins from the stage I to stage II, which results in an induced positive current in the coils. While a spinning of the rotator from stage II to stage III will lead to a continuous increase of the

DOI: 10.1021/acsnano.6b02384
ACS Nano XXXX, XXX, XXX−XXX

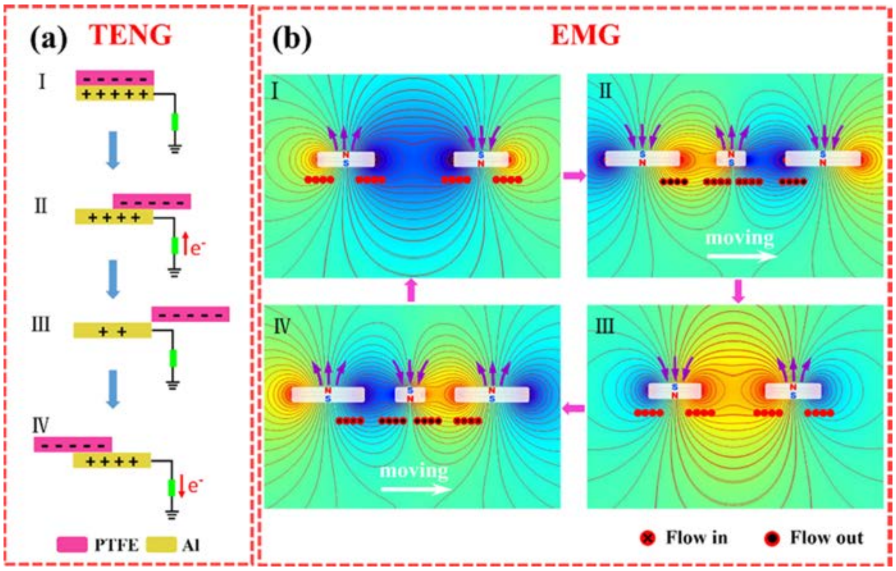

Figure 2. Working principle of the hybridized nanogenerator for power generation: (a) schematic diagram of working principle of TENG. The four process illustrate the charge distribution and electricity generation; (b) schematic diagram of working principle of EMG.

magnetic flux through the coils. With the rotator spins to stage IV, a decrease of the flux will induce a negative current in the coils. This is a full cycle of the electricity-generating process. An illustration of the rotator spinning is displayed in Supporting Figure S1 and Supporting Movie 1 in order to give a better view of the working principle of the device.

To characterize the hybridized nanogenerator for ambient mechanical energy harvesting, a first step was taken to study the output performance of the TENG. Figure 3a illustrates the dependence of the open-circuit voltage of TENG on the rotating speeds in a range from 10 to 1000 r/min. The voltages increase with the elevating rotation speeds until a saturated value of around 240 V, while a similar trend was also observed for the short-circuit current, and it is constant at around 10 μA, as demonstrated in Figure 3c. The output voltage and current of the TENG part at rotation rates higher than 500 rpm are respectively demonstrated in the Supporting Figure S2 panels a and b. Resistors were utilized as external loads to further investigate the output power of the TENG part for mechanical motions conversion. As displayed in Figure 3e, the current amplitude drops with increasing load resistances; as a result, the instantaneous peak power is maximized at a load resistance of 50 MΩ which corresponds to a peak power of 3.4 mW and a peak volume power density of 10.8 W/m^3. In addition, the stability test of the TENG was carried out at a rotational speed of 1000 rpm. On one hand, the open-circuit voltage and short-circuit current were measured before and after a 500 000 cycle continuous operation, and it is obvious that they all display little drops after 500 000 cycles of operation, as shown in Figure S3, panels a and b. On the other hand, all the two-output paramenters of the TENG that repeated on and off states over 1000 times were measured, and the open-circuit voltage and short-circuit current had no significant change, as shown in Figure S3c–f, which indicates good reliability and durability of the device for ambient mechanical energy harvesting.

Furthermore, the output performance of the EMG part was also characterized systematically. As shown in Figure 3 panels b and d, both the open-circuit voltage and short-circuit current of EMG is proportional to the external rotating speeds in a wide range from 10 to 1000 rpm, and respectively reach up to 7.5 V and 9 mA under the rotation rate of 1000 rpm, as the acquired signals displayed in Supporting Figure S2c,d. Moreover, the open-circuit voltage and short-circuit current decrease, while there is an increase in the distance between the magnets and coils, as shown in Figure S4. External resistances were also employed to evaluate the output performance of the EMG part of the hybridized nanogenerator. Figure 3f illustrates the dependence of the output current and power of the EMG on external resistances. And the largest instantaneous power of EMG is up to 16.2 mW at a loading resistance of 400 Ω, which corresponds to a volume output power density of 51.5 W/m^3. To evaluate the output power of a hybridized nanogenerator for ambient energy harvesting, the open-circuit voltage and short-circuit current of the device under excitation of environmental wind flow are shown in Supporting Figure S5.

To solve the critical impendence mismatch issue of the TENG and EMG, power management circuits were designed to bridge the electrical output of two parts, as illustrated in Figure 4a, and a transformer was employed to decrease the impendence of TENG. As shown in Figure 4b, the open-circuit voltage of TENG after using the transformers can be decreased to 7 V. Furthermore, to boost the total output current of the hybridized nanogenerator, two bridge rectification circuits were utilized to respectively convert the alternating current (AC) into direct current (DC). The output voltages from both the TENG and EMG are adjusted to a similar level, as shown in Figure 4c, when these two parts connected in parallel, the output voltage can maintain at 7 V. External resistances were also employed to evaluate the output performance of the hybridized nanogenerator. Figure 4d illustrates the dependence of the output current and power of the hybridized nanogenerator on external resistances. At a loading resistance of 700 Ω, an optimized instantaneous power of 17.5 mW was obtained. Figure 4 panels e and f illustrate the output voltage (3.5 V) and current (5 mA) of the hybridized nanogenerator at a loading resistance of 700 Ω.

To demonstrate the capacity of the hybridized nanogenerator as a practical power source, a G16 globe light is lit (Figure 5a, Supporting Movie 2) at a rotation rate of 1000 rpm, which is capable of providing sufficient illumination for reading text in complete darkness. Also, 12 G4 spot lights connected in parallel were also simultaneously lit (Figure 5b, Supporting Movie 3).

DOI: 10.1021/acsnano.6b02384
ACS Nano XXXX, XXX, XXX–XXX

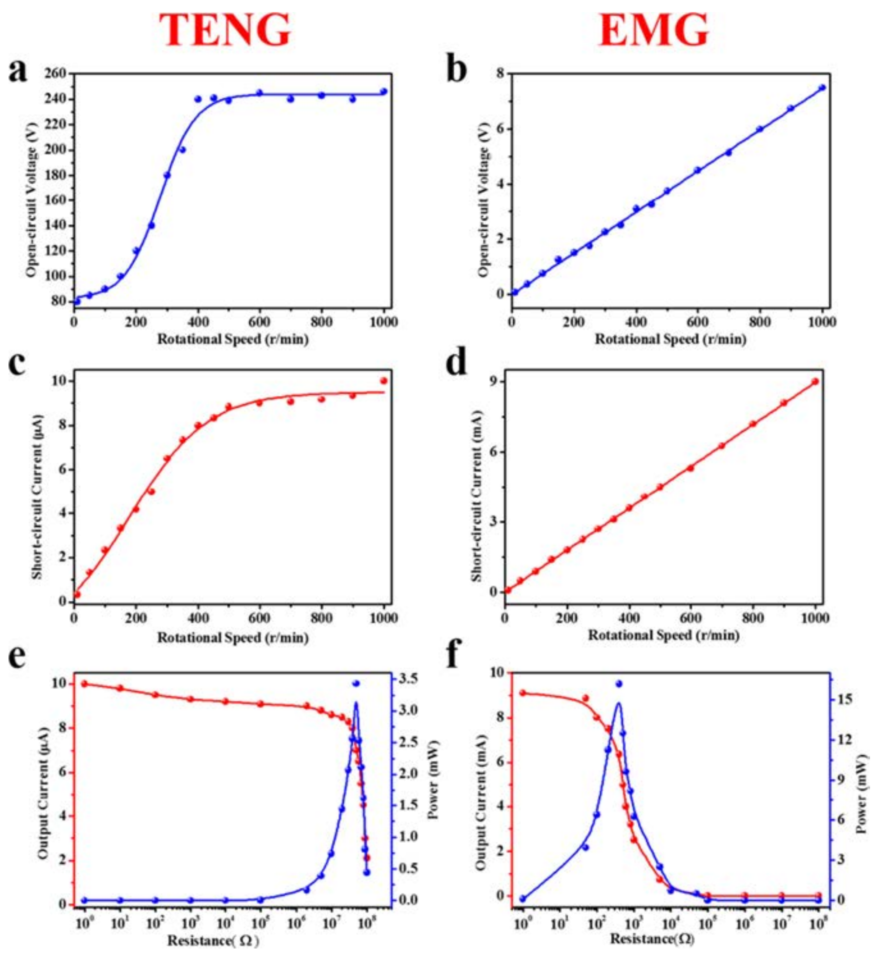

Figure 3. Electrical output performance of the TENG part and EMG part of the hybridized nanogenerator. (a, b) Dependence of the open-circuit voltage of TENG (a) and EMG (b) on rotating speeds ranging from 10 to 1000 rpm. (c, d) Short-circuit current of TENG (c) and EMG (d) with variable rotating speeds ranging from 10 to 1000 rpm. (e, f) Dependence of the output current and power of TENG (e) and EMG (f) on the external resistances.

In addition, this hybridized nanogenerator can harvest energy from a wind flow aroused from a motor vehicle going through tunnel. As displayed in Figure 5c,d, at a wind speed generated by a car moving nearly 8 m/s, this generator can light up a globe light (Supporting Movie 4 and Movie 5). The relationship of the rotational speed of the hybridized electromagnetic−triboelectric nanogenerator at different wind speeds is illustrated in Figure S6, and the hybridized nanogenerator was demonstrated to continuously power a wireless traffic volume sensor. Figure 5e is an illustration of the self-powered sensing system. The counter is triggered by a wireless transmitter powered by the hybridized nanogenerator by harvesting the wind flow energy from the passing by vehicles. The counter can display the times of the rotator running (Figure 5f, Supporting Movie 6). The self-powered wireless traffic volume sensor will greatly promote the development of real-time traffic volume monitoring, which will provide great convenience, especially in remote mountain areas.

CONCLUSION

In summary, we have demonstrated a rotating-disk-based hybridized nanogenerator as a self-powered wireless sensor for traffic volume monitoring in the remote mountain area. Under a rotating rate of 1000 rpm, the hybridized nanogenerator can deliver an instantaneous power of 17.5 mW for practical applications. At a loading of resistance of 700 Ω, the output voltage and current of the hybridized nanogenerator can reach respectively to 3.5 V and 5 mA. A counter was demonstrated to be triggered by a wireless transmitter that powered by the hybridized nanogenerator for real-time traffic volume monitoring, which is capable of providing great convenience to the traffic administration for real-time traffic-flow adjustment and effectively reduce the traffic problems. This invention of the self-powered active wireless traffic volume sensor will be of great importance to promote the development of ITS and provide a sustainable solution to the long-term continuous traffic volume monitoring in the remote area.

EXPERIMENTAL SECTION

Fabrication of the Nanowire Structures on the Surface of the PTFE Thin Film. A 50 μm thick PTFE thin film was cleaned with acetone, ethyl alcohol, and ultrapure water, consecutively, and then dried by compressed air. A thin Au film (10 nm), as the mask for etching the PTFE surface, was deposited on the PTFE surface using a DC sputter. Then, ICP reactive ion etching was utilized to produce nanoparticle-based modification on the surface of the PTFE film. Specifically, Ar, O_2, and CF_4 gases were introduced into the ICP chamber with the flow rates of 15, 10, and 30 sccm, respectively. One power source of 400 W was used to generate a high density of plasma, while another 100 W was used to accelerate the plasma ions. The PTFE thin film was etched for 10 s in order to produce particle-like nanostructures on the surface of PTFE film.

Fabrication of the Nanopore Structures on the Surface of the Aluminum Foil. First, the aluminum foil was cleaned with acetone,

DOI: 10.1021/acsnano.6b02384
ACS Nano XXXX, XXX, XXX−XXX

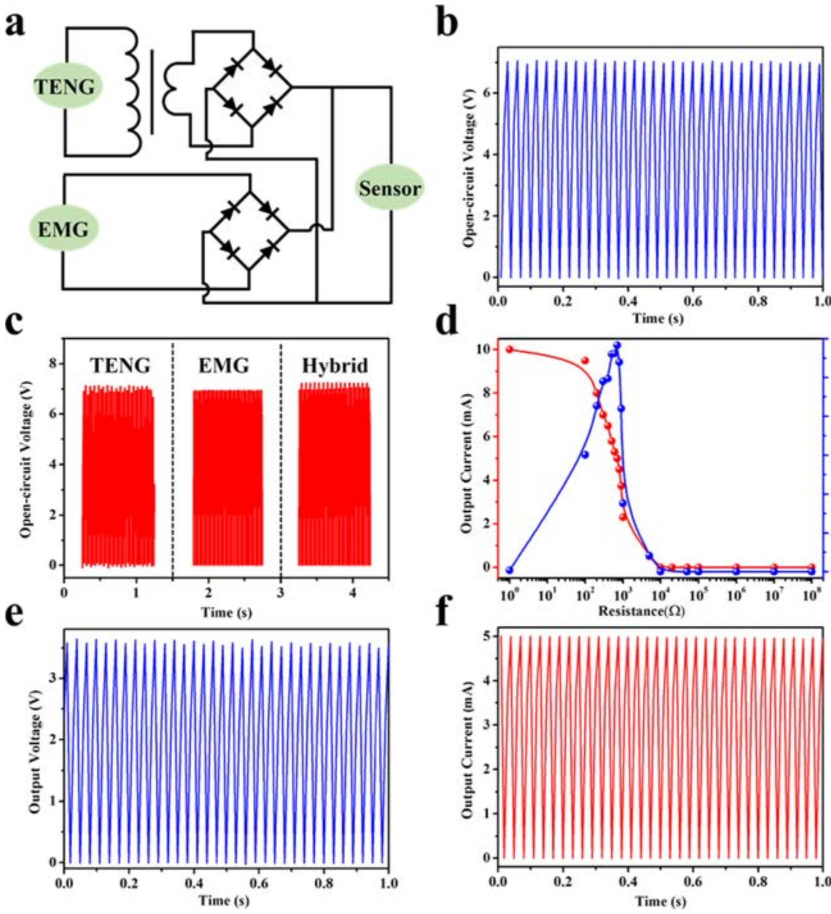

Figure 4. Schematic diagram and electrical output performance of the hybridized nanogenerator: (a) schematic diagram of the self-powered sensing system; (b) open-circuit voltage of TENG with transformer; (c) comparison of open-circuit voltage of TENG with transformer and rectification bridge, EMG with rectification bridge, and the hybridized nanogenerator; (d) dependence of the output current and power of the hybridized device on the external resistances; (e, f) output voltage (e) and current (f) of the hybridized nanogenerator at a loading resistance of 700 Ω.

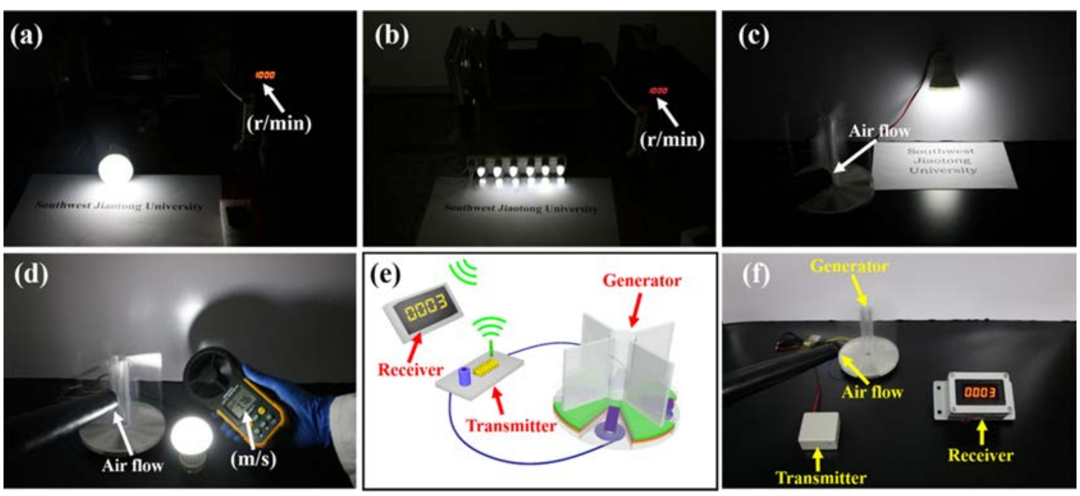

Figure 5. Demonstration of the hybridized nanogenerator as practical power sources and for a self-powered wireless traffic volume sensing system. (a, b) Photographs of a G16 globe light (a) and 12 G4 spot lights (b) that are directly powered by the hybridized nanogenerator in complete darkness (rotation rate: 1000 rpm). (c, d) A G16 globe light was powered for reading illumination in complete darkness by harvesting energy from fresh breeze at a flow speed of 7.76 m/s. (e, f) Schematic diagram (e) and photograph (f) of the wireless traffic volume sensing system that powered by the hybridized nanogenerator.

ethyl alcohol, and ultrapure water, consecutively, and then dried by compressed air. Then the Al foil was anodized in 2 mol L^{-1} phosphoric acid electrolyte. The first anodization was conducted under the constant anodization voltage of 180 V and electrolyte temperature of 3 °C. Then, the foil was immersed into a mixture of 6.0 wt/% H_3PO_4 and 1.8 wt/% H_2CrO_4 at 60 °C to remove the anodized layers. The nanopores array

DOI: 10.1021/acsnano.6b02384
ACS Nano XXXX, XXX, XXX−XXX

were obtained by the second anodization at constant voltage of 180 V at 3 °C electrolyte temperature.

Fabrication of the Hybridized Electromagnetic-Triboelectric Nanogenerator. First, two 2 mm thick acrylic sheets were processed by laser cutting (TR-6040) to form the two cyclostyles as supporting substrates. The tailored PTFE and PU films and aluminum foil with radial arrayed structure were attached onto the acrylic loading templates. Four magnets and four groups of coils were respectively embedded in the acrylic substrate with physical gap in between.

Electrical Measurement. The open-circuit voltage was measured by using a Keithley 6514 system electrometer, and the short-circuit current was measured by using an SR570 low noise current amplifier (Stanford Research System).

ASSOCIATED CONTENT

Supporting Information

The Supporting Information is available free of charge on the ACS Publications website at DOI: 10.1021/acsnano.6b02384.

spinning rotator (AVI)
lighting of a G16 globe light (AVI)
lighting of 12 G4 spot lights connected in parallel (AVI)
nanogenerator harvesting energy from a wind flow (AVI)
nanogenerator harvesting energy from a wind flow (AVI)
wireless traffic volume sensing system (AVI)
detailed calculation of the volume power density; list that ranks materials according to their tendency to gain or lose electrons; additional figures (PDF)

AUTHOR INFORMATION

Corresponding Authors

*E-mail: wqyang@swjtu.edu.cn.
*E-mail: zlwang@gatech.edu.

Author Contributions

#Binbin Zhang and Jun Chen contributed equally to this work.

Notes

The authors declare no competing financial interest.

ACKNOWLEDGMENTS

This work is supported by the scientific and technological projects for Distinguished Young Scholars of Sichuan Province (No.2015JQ0013), the Fundamental Research Funds for the Central Universities of China (A0920502051408), the independent Research Project of State Key Laboratory of Traction Power (No. 2016TPL_Z03), the Hightower Chair foundation, and the "thousands talents" program for pioneer researcher and his innovation team, China. Patents have been filed based on the research results presented in this manuscript.

REFERENCES

(1) Taniguchi, E.; Shimamoto, H. Intelligent Transportation System Based Dynamic Vehicle Routing and Scheduling with Variable Travel Times. *Transport. Res. C-Emer.* **2004**, *12*, 235−250.

(2) Andrisano, O.; Verdone, R.; Nakagawa, M. Intelligent transportation systems: The Role of Third Generation Mobile Radio Networks. *IEEE Commun. Mag.* **2000**, *38*, 144−151.

(3) Han, M.; Zhang, X.; Sun, X.; Meng, B.; Liu, W.; Zhang, H. X. Magnetic-Assisted Triboelectric Nanogenerators as Self-Powered Visualized Omnidirectional Tilt Sensing System. *Sci. Rep.* **2014**, *4*, 4811−4811.

(4) Yang, W.; Chen, J.; Wen, X. N.; Jing, Q. S.; Yang, J.; Wei, X. N.; Su, Y. J.; Zhu, G.; Wu, W. Z.; Wang, Z. L. Triboelectrification Based Motion Sensor for Human-Machine Interfacing. *ACS Appl. Mater. Interfaces* **2014**, *6*, 7479−7484.

(5) Zhu, G.; Yang, W.; Zhang, T.; Jing, Q. S.; Chen, J.; Zhou, Y. S.; Bai, P.; Wang, Z. L. Self-Powered, Ultrasensitive, Flexible Tactile Sensors Based on Contact Electrification. *Nano Lett.* **2014**, *14*, 3208−3213.

(6) Su, Y.; Zhu, G.; Yang, W.; Yang, J.; Chen, J.; Jing, Q.; Wu, Z.; Jiang, Y.; Wang, Z. L. Triboelectric Sensor for Self-Powered Tracking of Object Motion inside Tubing. *ACS Nano* **2014**, *8*, 3843−3850.

(7) Zhu, G.; Chen, J.; Zhang, T.; Jing, Q.; Wang, Z. L. Radial-Arrayed Rotary Electrification for High Performance Triboelectric Generator. *Nat. Commun.* **2014**, *5*, 487−507.

(8) Chen, J.; Yang, J.; Li, Z.; Fan, X.; Zi, Y.; Jing, Q.; Guo, H.; Wen, Z.; Pradel, K. C.; Niu, S.; Wang, Z. L. Networks of Triboelectric Nanogenerators for Harvesting Water Wave Energy: A Potential Approach toward Blue Energy. *ACS Nano* **2015**, *9*, 3324−3331.

(9) Zhang, L.; Jin, L.; Zhang, B.; Deng, W.; Pan, H.; Tang, J.; Zhu, M.; Yang, W. Q. Multifunctional Triboelectric Nanogenerator Based on Porous Micro-Nickel Foam to Harvest Mechanical Energy. *Nano Energy* **2015**, *16*, 516−523.

(10) Yang, J.; Chen, J.; Liu, Y.; Yang, W. Q.; Su, Y. J.; Wang, Z. L. Triboelectrification-Based Organic Film Nanogenerator for Acoustic Energy Harvesting and Self-Powered Active Acoustic Sensing. *ACS Nano* **2014**, *8*, 2649−2657.

(11) Yang, W. Q.; Chen, J.; Zhu, G.; Yang, J.; Bai, P.; Su, Y. J.; Jing, Q. S.; Cao, X.; Wang, Z. L. Harvesting Energy from the Natural Vibration of Human Walking. *ACS Nano* **2013**, *7*, 11317−11324.

(12) Yang, W. Q.; Chen, J.; Jing, Q. S.; Yang, J.; Wen, X. N.; Su, Y. J.; Zhu, G.; Bai, P.; Wang, Z. L. 3D Stack Integrated Triboelectric Nanogenerator for Harvesting Vibration Energy. *Adv. Funct. Mater.* **2014**, *24*, 4090−4096.

(13) Chen, J.; Zhu, G.; Yang, W. Q.; Jing, Q. S.; Bai, P.; Yang, Y.; Hou, T. C.; Wang, Z. L. Harmonic-Resonator-based Triboelectric Nanogenerator as a Sustainable Power Source and a Self-Powered Active Vibration Sensor. *Adv. Mater.* **2013**, *25*, 6094−6099.

(14) Yang, J.; Chen, J.; Yang, Y.; Zhang, H. L.; Yang, W. Q.; Bai, P.; Su, Y. J.; Wang, Z. L. Broadband Vibrational Energy Harvesting Based on a Triboelectric Nanogenerator. *Adv. Energy Mater.* **2014**, *4*, 590−592.

(15) Yang, W.; Chen, J.; Zhu, G.; Wen, X. N.; Bai, P.; Su, Y. J.; Lin, Y.; Wang, Z. L. Harvesting Vibration Energy by a Triple-Cantilever Based Triboelectric Nanogenerator. *Nano Res.* **2013**, *6*, 880−886.

(16) Zhang, L.; Zhang, B.; Chen, J.; Jin, L.; Deng, W.; Tang, J.; Zhang, H.; Pan, H.; Zhu, M. H.; Yang, W. Q.; Wang, Z. L. Lawn Structured Triboelectric Nanogenerators for Scavenging Sweeping Wind Energy on Rooftop. *Adv. Mater.* **2016**, *28*, 1650−1656.

(17) Chen, J.; Zhu, G.; Yang, J.; Jing, Q.; Bai, P.; Yang, W.; Qi, X.; Su, Y.; Wang, Z. L. Personalized Keystroke Dynamics for Self-Powered Human-Machine Interfacing. *ACS Nano* **2015**, *9*, 105−116.

(18) Wen, X. N.; Yang, W. Q.; Jing, Q. S.; Wang, Z. L. Harvesting Broadband Kinetic Impact Energy from Mechanical Triggering/Vibration and Water Waves. *ACS Nano* **2014**, *8*, 7405−7412.

(19) Chen, J.; Yang, J.; Guo, H.; Li, Z.; Zheng, L.; Su, Y.; Wen, Z.; Fan, X.; Wang, Z. L. Automatic Mode Transition Enabled Robust Triboelectric Nanogenerators. *ACS Nano* **2015**, *9*, 12334−12343.

(20) Zhang, K.; Wang, X.; Yang, Y.; Wang, Z. L. Hybridized Electromagnetic-Triboelectric Nanogenerator for Scavenging Biomechanical Energy for Sustainably Powering Wearable Electronics. *ACS Nano* **2015**, *9*, 3521−3529.

(21) Fan, X.; Chen, J.; Yang, J.; Bai, P.; Li, Z.; Wang, Z. L. Ultrathin, Rollable, Paper-Based Triboelectric Nanogenerator for Acoustic Energy Harvesting and Self-Powered Sound Recording. *ACS Nano* **2015**, *9*, 4236−4243.

(22) Wang, Z. L.; Chen, J.; Lin, L. Progress in Triboelectric Nanogenerators as a New Energy Technology and Self-Powered Sensors. *Energy Environ. Sci.* **2015**, *8*, 2250−2282.

(23) Yang, J.; Chen, J.; Su, Y.; Jing, Q.; Li, Z.; Yi, F.; Wen, X.; Wang, Z.; Wang, Z. L. Eardrum- Inspired Active Sensors for Self-Powered Cardiovascular System Characterization and Throat-Attached Anti-Interference Voice Recognition. *Adv. Mater.* **2015**, *27*, 1316−1326.

(24) Guo, H.; Chen, J.; Yeh, M. H.; Fan, X.; Wen, Z.; Li, Z.; Hu, C.; Wang, Z. L. An Ultrarobust High-Performance Triboelectric Nano-

generator Based on Charge Replenishment. *ACS Nano* **2015**, *9*, 5577−5584.
(25) Fang, H.; Wu, W.; Song, J.; Wang, Z. L. Controlled Growth of Aligned Polymer Nanowires. *J. Phys. Chem. C* **2011**, *113*, 16571−16574.
(26) Wen, Z.; Chen, J.; Yeh, M. H.; Guo, H.; Li, Z.; Fan, X.; Zhang, T.; Zhu, L.; Wang, Z. L. Blow-Driven Triboelectric Nanogenerator as an Active Alcohol Breath Analyzer. *Nano Energy* **2015**, *16*, 38−46.
(27) Su, Y.; Chen, J.; Wu, Z.; Jiang, Y. Low Temperature Dependence of Triboelectric Effect for Energy Harvesting and Self-Powered Active Sensing. *Appl. Phys. Lett.* **2015**, *106*, 013114.
(28) Zhu, G.; Chen, J.; Liu, Y.; Bai, P.; Zhou, Y. S.; Jing, Q.; Pan, C.; Wang, Z. L. Linear- Grating Triboelectric Generator Based on Sliding Electrification. *Nano Lett.* **2013**, *13*, 2282−2289.
(29) Zhu, G.; Bai, P.; Chen, J.; Wang, Z. L. Power-Generating Shoe Insole Based on Triboelectric Nanogenerators for Self-Powered Consumer Electronics. *Nano Energy* **2013**, *2*, 688−692.
(30) Su, Y.; Wen, X.; Zhu, G.; Yang, J.; Chen, J.; Bai, P.; Wu, Z.; Jiang, Y.; Wang, Z. L. Hybrid Triboelectric Nanogenerator for Harvesting Water Wave Energy and as a Self-Powered Distress Signal Emitter. *Nano Energy* **2014**, *9*, 186−195.
(31) Li, Z.; Chen, J.; Yang, J.; Su, Y.; Fan, X.; Wu, Y.; Yu, C.; Wang, Z. L. β-Cyclodextrin Enhanced Triboelectrification for Self-Powered Phenol Detection and Electrochemical Degradation. *Energy Environ. Sci.* **2015**, *8*, 887−896.
(32) Zhu, G.; Peng, B.; Chen, J.; Jing, Q.; Wang, Z. L. Triboelectric Nanogenerators as a New Energy Technology: From Fundamentals, Devices, to Applications. *Nano Energy* **2015**, *14*, 126−138.
(33) Zi, Y.; Lin, L.; Wang, J.; Wang, S.; Chen, J.; Fan, X.; Yang, P. K.; Yi, F.; Wang, Z. L. Triboelectric-Pyroelectric-Piezoelectric Hybrid Cell for High-Efficiency Energy-Harvesting and Self-Powered Sensing. *Adv. Mater.* **2015**, *27*, 2340−2347.

DOI: 10.1021/acsnano.6b02384
ACS Nano XXXX, XXX, XXX−XXX